Available online at www.sciencedirect.com

ScienceDirect

Procedia Computer Science 91 (2016) 372 – 381

Procedia Computer Science

Information Technology and Quantitative Management (ITQM2016)

Modeling electrostatic separation process using artificial neural network (ANN)

Koon Chun Lai[a,*], Soo King Lim[b], Peh Chiong Teh[a], Kim Ho Yeap[a]

[a]Faculty of Engineering and Green Technology, Universiti Tunku Abdul Rahman, Kampar Campus, 31900 Perak, Malaysia
[b]*LKC Faculty of Engineering and Science, Universiti Tunku Abdul Rahman, Sungai Long Campus, 43000 Selangor, Malaysia*

Abstract

In this paper, the characteristics of an electrostatic separator were modeled using artificial neural network (ANN). The model was constructed by considering the misclassified middling product during separation, where system parameters (voltage level, rotation speed, electrode position, etc) were varied. The ANN architecture was optimized through the variation in the neuron number, percentage of testing data and percentage of validation data. Performance of the network was assessed by the error indicators, namely mean square error (MSE) and coefficient of determination (R-square). It is found that, lesser number of neurons and lower percentage of both training and validation dataset contributes to better network performance. Additionally, network architecture thus derived was selected for a detailed study on the various combinations performance corresponding to the input and output variables. The results consequently suggest a simplified network structure with reduced number of input variables for modeling of this nonlinear process.

Peer-review under responsibility of the Organizing Committee of ITQM 2016

Keywords: electrostatic separator; mean square error; coefficient of determination; artificial neural network

1. Introduction

Owing to the induced corona and electrostatic forces, electrostatic separator is a high voltage driven apparatus to sort two or more substances with different electrical conductivity. Typically, the roll-type separator comprises a rotating roller, a feeder, corona and electrostatic electrodes as well as a DC high voltage power supply. It was initially used in food security industry, e.g. to remove hairs or waste straws during packaging process [1], and consequently employed in the fields of metal recovery from printed-circuit board waste [2], ash removal [3], and lately in waste recycling domain [4] to reduce landfill due to improper waste disposal way [5].

* Corresponding author. Tel.: +605-4688888; fax: +605-4667449.
E-mail address: laikc@utar.edu.my

Peer-review under responsibility of the Organizing Committee of ITQM 2016
doi:10.1016/j.procs.2016.07.099

Medles et al. reported the model of electrostatic separation process. They sorted the electric cable wastes which consist of 5 % copper and 95 % PVC. A quadratic polynomial function was proposed to predict the optimal set point of the process based on the input factors of high voltage level, roll electrode rotating speed and the splitter angular position [6]. Dascalescu et al. reported the response surface model by considering the factors of mixtures characteristics, the feed rate, electrodes configuration and the applied voltage [7]. In the above referred model, the sample is a mixture of conductive and non-conductive materials, which differed by the electrical conductivity [8]. Lately, Bilici et al. reported the behavioral model of polymer mixture separation and found the particles charge/mass ratio affect the separating outcomes [9]. Aryafard et al. proposed an integrated process model of electrostatic separation [10]. Tripathy et al. reported a mathematical model based on the factorial design combined with response surface methodology. It is found that the temperature, feed rate and rolling speed have influences on both the recovery and grade of the separation process [11].

The literatures revealed that the electrostatic separation is a complicated process involving a number of process inputs. Thus it is an urge to find out a comprehensive model for the evaluating and experimentation purposes. This present study reports artificial neural network (ANN) for modeling of the separation process. The proposed ANN is built with nonlinear sigmoid functions based on a Levenberg-Marquardt backpropagation method, so as to model the parameters such as voltage level, rolling speed and electrodes position. The implementations of ANN in the field of nonlinear process modeling have become popular recently [12]. However, to the best of our knowledge, there are few researches made on the electrostatic separator using ANN. The target of this study is as follows: after the brief introduction, forces induced during the separation process were discussed, followed by construction and implementation of ANN. Detailed results and discussion on the optimized ANN architecture were subsequently reported before the final conclusion was made at the end of this paper.

2. Electrostatic separation process

Electrostatic separation sorts two different types of substances with different electrical conductivity at once. Prior to the electrostatic separation, the substances are typically charged by friction charge, induced charge or corona charge before subjecting to the electrostatic and gravity forces. In the waste processing industry, the corona charging separator can be used to recover copper from used electrical wire, or to separate scrap papers from the paper-plastic mixture. This technique is free from pollution as it does not involve burning or chemical reaction.

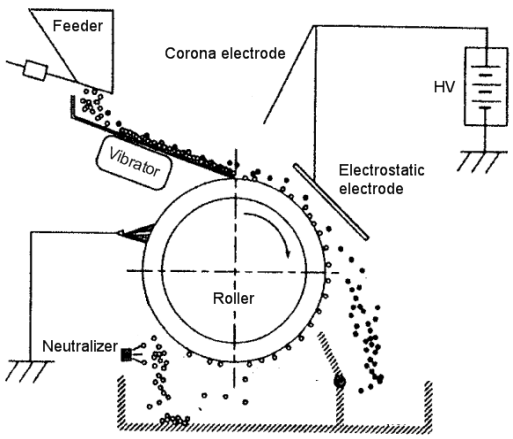

Fig. 1. Corona charging type electrostatic separator [1]

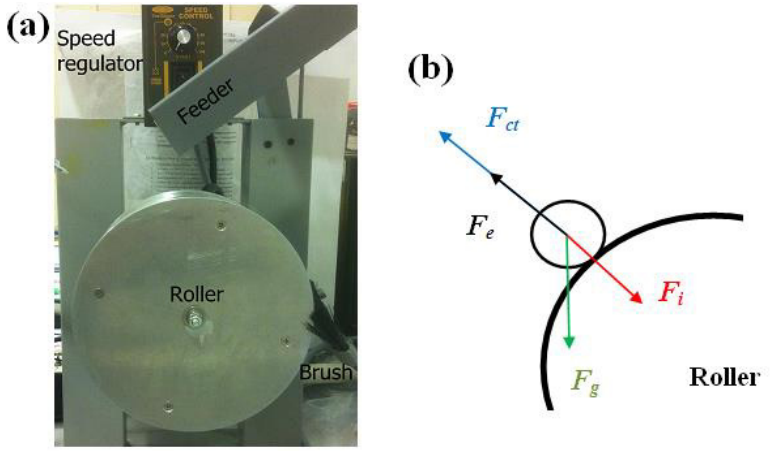

Fig. 2. Electrostatic separation process: (a) test rig; (b) forces act on particles

As demonstrated in Fig. 1, the substances on the roller surface are subjected to electric charge ionized from the needle corona electrode and eventually separated due to the differences in conductivity and electrostatic properties. Electrostatic separation process relies on the forces act on the particles, which includes the (i) centrifugal force due to the rotation, (ii) lifting force due to the attraction by electrostatic electrode, (iii) gravity force, and (iv) pinning force due to the ion generation from the corona electrode. The test rig of the separator and forces act on particles are illustrated in Fig. 2. The particles that pass through the corona ionizing zone are subjected to ionizing and pinning effects generated by the corona electrode. According to [13], the induced pinning force, or known as image force, F_i correlates to the size of the particles and is defined as:

$$F_i = \frac{Q^2}{4\pi \cdot d^2 \varepsilon} \tag{1}$$

where Q is particle charge, d is the particle thickness and ε is dielectric constant of particle. The electrostatic electrode located downstream the corona electrode induces a lifting force, the strength of which relies on the electric field. The lifting force, also known as electrostatic force, F_e, applied on the particles was calculated by:

$$F_e = QE \tag{2}$$

where E is the electric field strength. Besides, the gravity force, F_g, acted on the mass, m, of the particles was defined as:

$$F_g = mg = \rho A d \cdot g \tag{3}$$

where A is the surface area of particle and ρ is the density of the particle. The centrifugal force applied on the particles is generated by the roller which rotates in counter-clockwise angular direction. This force, F_{ct}, is always at an opposite direction to that of the pinning force and computed as [14]:

$$F_{ct} = m\omega^2 R \tag{4}$$

where R is the radius of roller and ω is the angular rotating velocity. Due to the force effect, the separator sorts the more conductive matter and less conductive matter to different collection tanks. Some matter may fall in between as middling product, resulting in a decline in separation efficiency.

3. ANN modeling and implementation

An artificial neural network is viewed as a numerical estimation method to simulate the learning and memorizing operation. It is a powerful tool that learns through the experimental input variables and determines the governing rules between the corresponding factors [15]. The structure of a multi-layer feed forward network developed in MATLAB is shown in Fig. 3. ANN has an input layer, an output layer and a hidden layer to compute the complex interconnections of neurons intelligently. Neurons are the constitutive units of the artificial neural network. It receives one or more inputs and sums them to generate an output through an activation function. In this study nonlinear sigmoid activation function is used in the hidden layer. The network accepts a number of inputs (denoted by n) and the targeted output for training. There are three stages namely training, testing and validation performed by the network. Typically by random sampling method, about 70% experimental data is used for training, 15% for validation, and rest of data for testing [16]. Random initial weights are assigned to each of the inputs as the first step, and the weights would change by the Levenberg-Marquardt backpropagation training algorithm. The training stops when the satisfactory results are achieved. At this stage the results move in the forward direction from the hidden layer toward the output layer which has a linear activation function. A validation process is performed to adjust the combination through a number of iterations and to generate the reasonable parameters for learning algorithm. The network is then tested in order to assess the prediction accuracy in a measurement of mean squared error (MSE), which is determined by:

$$\mathrm{MSE} = \frac{\sum_{i=1}^{n} (t_i - y_i)^2}{n} \tag{5}$$

where t is target value and y is output value. In the present study, the neural network is configured as a multiple input-single output (MISO) model in the MATLAB environment. Considering the abovementioned literatures, six design factors namely voltage level of the DC power supply (kV), rotation speed of the roller (rpm), ambient temperature (degree C), electrode configurations i.e. corona electrode angle (degree), corona electrode distance from roller surface (mm) and electrostatic electrode distance from roller surface (mm) are considered as inputs, whereas the middling product mass (g) is selected as net output.

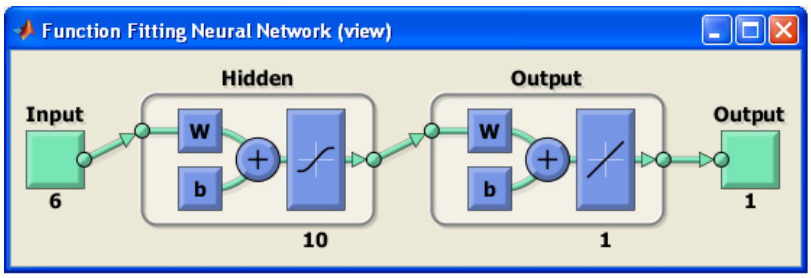

Fig. 3. ANN structure used for modeling

Table 1. Separation parameters and their levels

Parameter	Unit	Level of parameter	
		Low	High
Voltage level	kV	20	30
Rotation speed	rpm	60	90
Temperature	degree C	24	28
Corona electrode angle	degree	30	50
Corona electrode distance	mm	50	60
Electrostatic electrode distance	mm	40	50

Two levels factorial design is taken into consideration for the experimentation, as shown in Table 1. A total of 64 net output variables could be generated, and they change when the training, test and validation data are varied. Network efficiency would be enhanced with the optimum percentage of data in the three stages and number of hidden neurons. The best performance of the ANN architecture is determined by the lowest MSE and the maximum coefficient of determination (R-squared) that defines the fit integrity of experimental data.

$$R^2 = 1 - \frac{\sum_{i=1}^{n}(t_i - y_i)^2}{\sum_{i=1}^{n}(y_i)^2} \tag{6}$$

4. Results and discussion

Fig. 4 depicts the simulation results corresponding to predicted and target data. Result of the scatter plot shows acceptable prediction with less than 0.1 differences between predicted and target data based on the correlation equation. In order to judge the extrapolating capability, performances of ANN relate to variation in neuron number, testing and validation dataset are further analyzed in this paper.

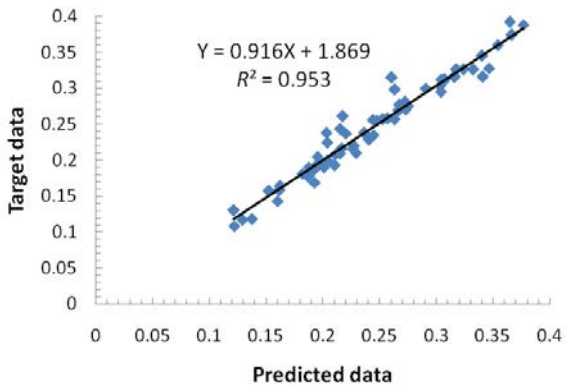

Fig. 4. Comparison of predicted data with target data

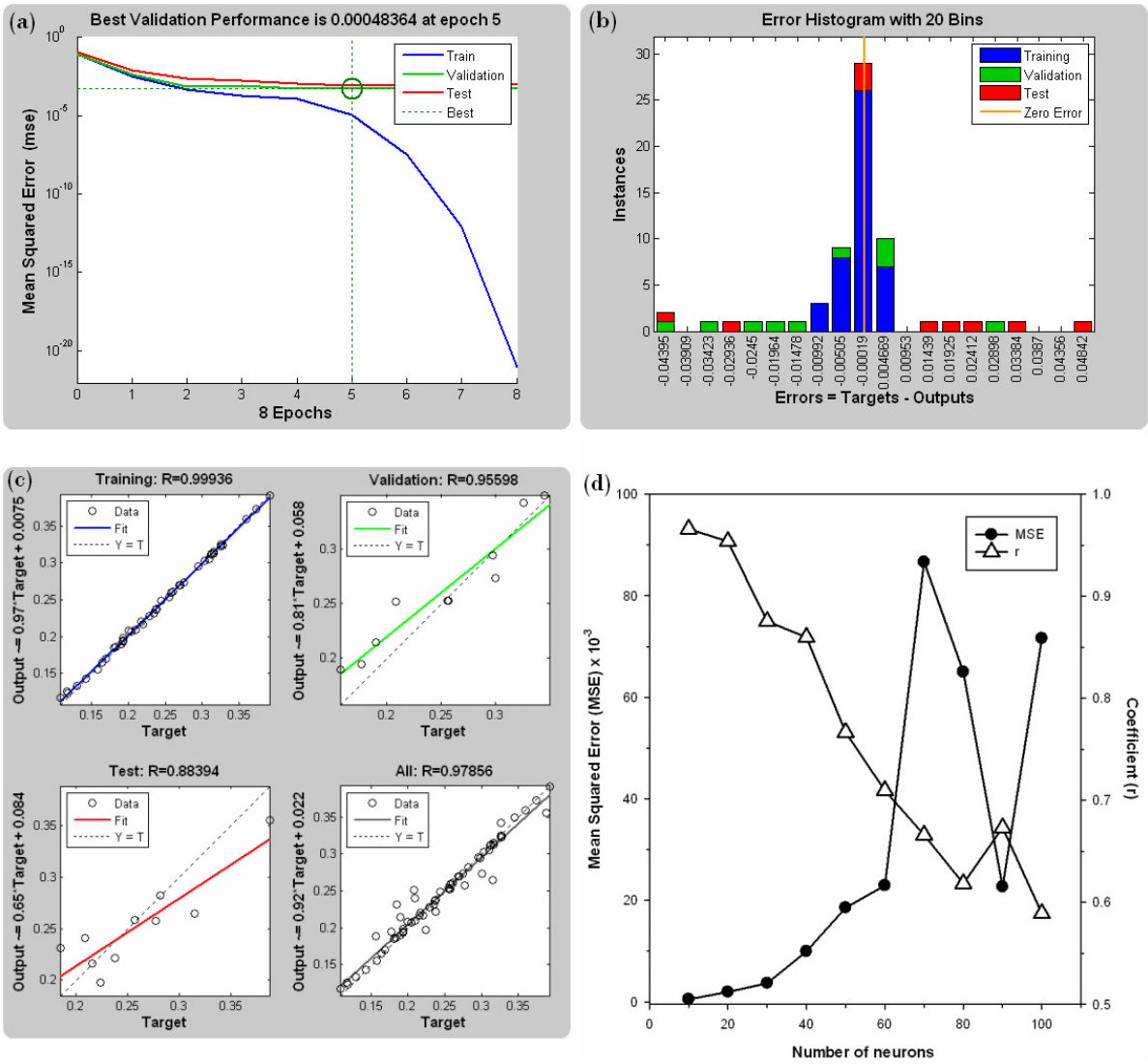

Fig. 5. Neural network performance. (a) MSE between training, validation and testing; (b) errors between training, validation and testing; (c) R-squared between target value and output value; (d) variation in number of neurons and corresponding MSE and R-squared

Fig. 5(a)-(d) show the performance of neural network due to variation in the number of neurons at constant percentage of testing and validation data. Table 2 tabulates the performance in terms of mean squared error (MSE) and coefficient of determination (R-squared) when the number of neurons is increased from 10 to 100. It is noted that MSE increases and R-squared value decreases at larger number of neurons. Fig. 5(a) shows the MSE between training, testing and validation data with 10 neurons in hidden layer. It is found in this case that MSE is determined as 4.8364×10^{-4} at epoch 5. Fig. 5(b) presents the corresponding error histogram. Along the same lines, R-squared value is found to be 0.9577 in Fig. 5(c). Fig. 5(d) summarizes the response of variation in MSE and correlation (R) with different number of neurons, while keeping both validation data percentage

and testing data percentage at 15%. It is noted that performance becomes worse at higher number of neurons, which in other word, implies that lower number of hidden neurons should be used in modeling so as to produce the minimum MSE and higher value of R-squared.

In order to examine the effect of testing data, on the other hand, the percentage of testing data is varied from 5% to 35% while keeping the percentage of validation data constant at 5%. The network performances are summarized in Table 3. It is found that the minimum MSE is 4.0415×10^{-5} at epoch 14 at lower percentage of testing data as shown in Fig 6(a). Fig. 6(b) and (c) present the error histogram and correlation (R). The results of variation in the testing data, as shown in Fig. 6(d), evidently show the minimal MSE and maximal R-squared would exist at lower number of testing data.

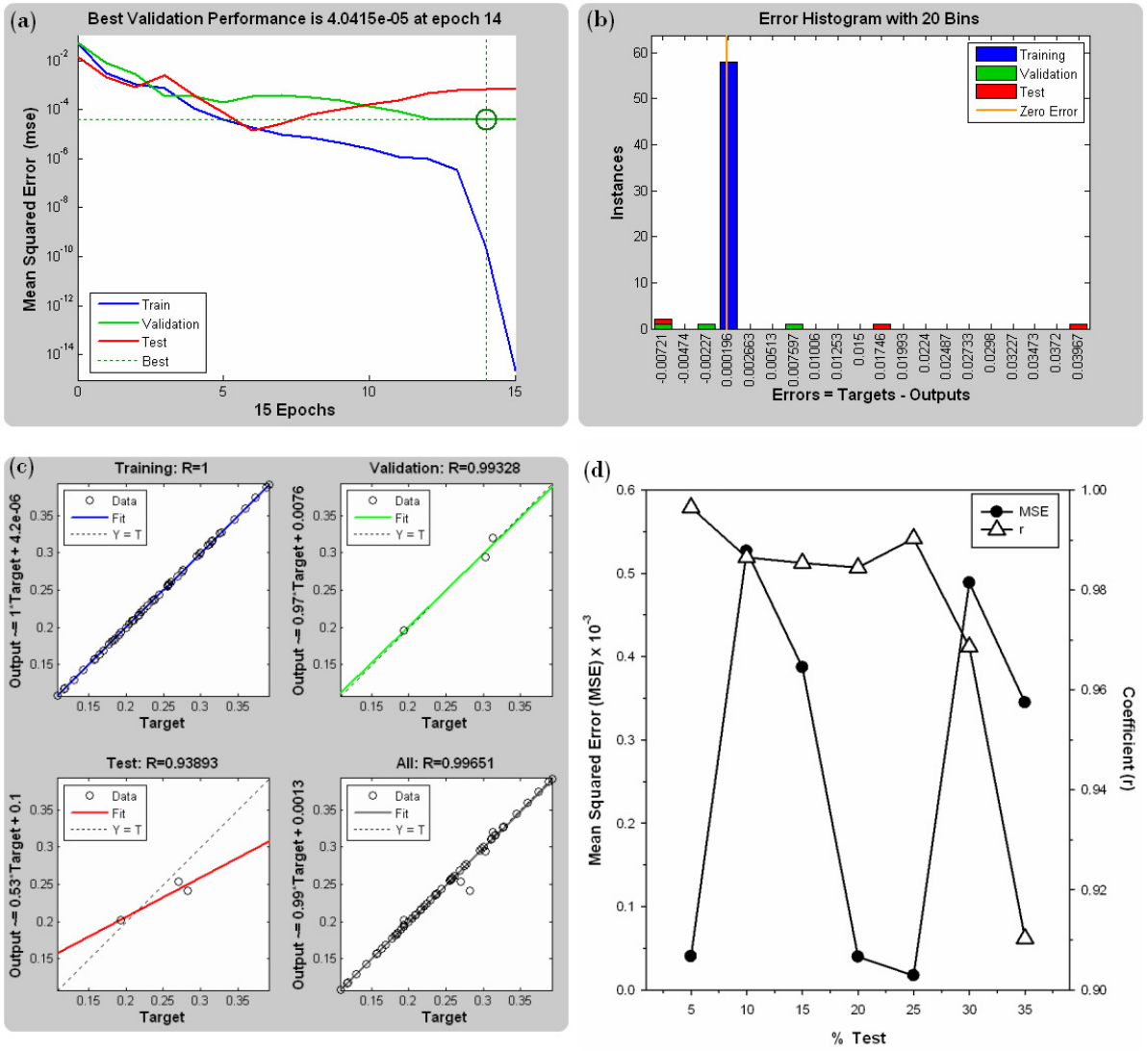

Fig. 6. Neural network performance. (a) MSE between training, validation and testing; (b) errors between training, validation and testing; (c) R-squared between target value and output value; (d) variation in number of test data and corresponding MSE and R-squared

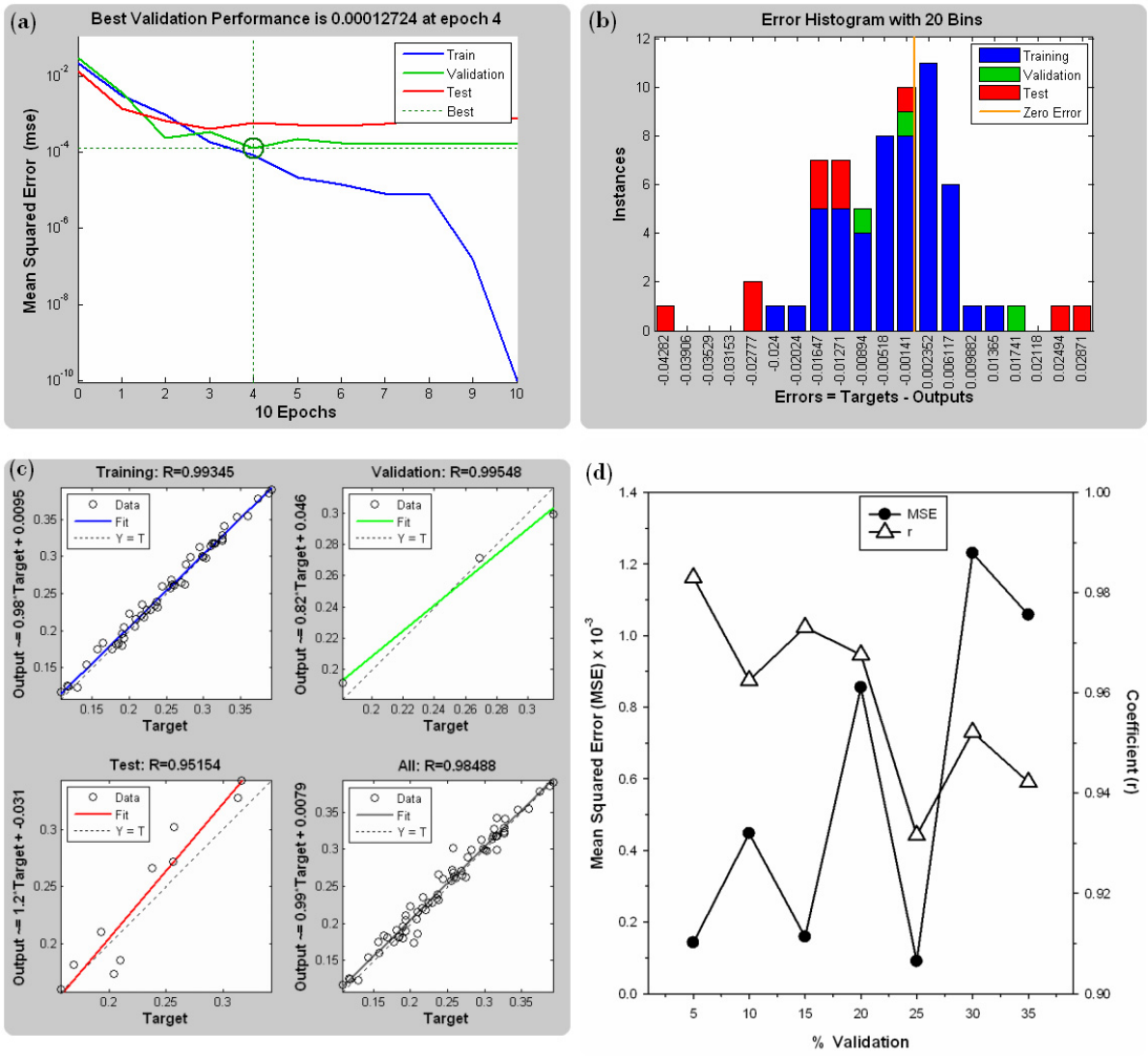

Fig. 7. Neural network performance. (a) MSE between training, validation and testing; (b) errors between training, validation and testing; (c) R-squared between target value and output value; (d) variation in number of validation data and corresponding MSE and R-squared

Likewise, percentage of validation data is varied from 5% to 35% and the results are tabulated in Table 4. Fig. 7(a)-(c) show the MSE, error histogram and correlation (R). Fig. 7(d) further presents the response of variation in the validation data. The results suggested that minimal MSE and maximal R-squared would exist at lower number of validation data.

The optimized ANN structure is selected for a detailed study on the various combinations performance corresponding to the input and output variables. This is for a conservative case when the complete set of input variables are not taken into account in ANN. Therefore when some input variables are absent, the network is still able to give accurate estimates for the output through the complex relationship between the variables which were prior determined.

Table 2. Variation in the number of hidden neurons

% Validation	% Testing	Neurons	MSE	R-squared
15	15	10	4.8364×10^{-4}@ epoch 5	0.9577
15	15	20	1.9530×10^{-3}@ epoch 2	0.9097
15	15	30	3.6761×10^{-3}@ epoch 5	0.7663
15	15	40	9.9226×10^{-3}@ epoch 4	0.7394
15	15	50	1.8550×10^{-2}@ epoch 4	0.5877
15	15	60	2.2927×10^{-2}@ epoch 4	0.5035
15	15	70	8.6645×10^{-2}@ epoch 4	0.4437
15	15	80	6.4990×10^{-2}@ epoch 4	0.3824
15	15	90	2.2666×10^{-2}@ epoch 2	0.4532
15	15	100	7.1599×10^{-2}@ epoch 3	0.3473

Table 3. Variation in the number of testing data

% Validation	% Testing	Neurons	MSE	R-squared
5	5	10	4.0415×10^{-5}@ epoch 14	0.9930
5	10	10	5.2664×10^{-4}@ epoch 7	0.9732
5	15	10	3.8715×10^{-4}@ epoch 3	0.9710
5	20	10	3.9614×10^{-5}@ epoch 6	0.9692
5	25	10	1.7158×10^{-5}@ epoch 4	0.9807
5	30	10	4.8852×10^{-4}@ epoch 4	0.9382
5	35	10	3.4475×10^{-4}@ epoch 6	0.8286

Table 4. Variation in the number of validation data

% Validation	% Testing	Neurons	MSE	R-squared
5	15	10	1.2724×10^{-4}@ epoch 4	0.9700
10	15	10	4.4746×10^{-4}@ epoch 5	0.9264
15	15	10	1.5877×10^{-4}@ epoch 3	0.9469
20	15	10	8.5504×10^{-4}@ epoch 4	0.9362
25	15	10	9.0426×10^{-4}@ epoch 4	0.8679
30	15	10	1.2300×10^{-3}@ epoch 3	0.9067
35	15	10	1.0580×10^{-3}@ epoch 7	0.8877

Table 5. Various input combinations (hidden neurons: 10, %Testing: 15, %Validation: 15)

Simulation	Inputs	MSE	R-squared
1	Voltage level – rotation speed – temperature	5.4852×10^{-4}	0.9123
2	Voltage level – rotation speed – corona electrode angle	3.3871×10^{-4}	0.9482
3	Voltage level – rotation speed – corona electrode distance	4.1816×10^{-4}	0.9331

Table 5 presents the simulation for selected combination of inputs and middling as output. As can be seen, voltage level – rotation speed – corona electrode angle combination has less MSE and higher R-squared value, indicating the best combination than others with middling as output. Its error indicators, namely MSE and R-squared, are 3.3871×10^{-4} and 0.9482 respectively. This implies that, the above combination which would require fewer inputs can be used in a simplified ANN structures for modeling the electrostatic separation process as for time and cost saving measures.

5. Conclusion

A model of electrostatic separation process using artificial neural network was reported in this paper. Simulation results suggest the use of lower number of neurons, test and validation dataset for accurate prediction. Values of error indicators for the network are low, indicating a less deviation between the predicted and target data. This shows that ANN is a potential preeminent tool to model nonlinear processes such as electrostatic separation.

References

[1] Masui N. Electrostatic separation for removal from green tea of stems and from food of impurities. *Proceedings of the IEJ* 1982; **6(3)**: 159-162.
[2] Veit HM, Diehl TR, Salami AP, Rodrigues JS, Bernardes AM., Tenório JAS. Utilization of magnetic and electrostatic separation in the recycling of printed circuit boards scrap. *Waste management* 2005; **25(1)**: 67-74.
[3] Mohanta SK, Rout B, Dwari RK, Reddy PSR, Mishra BK. Tribo-electrostatic separation of high ash coking coal washery rejects: Effect of moisture on separation efficiency. *Powder Technology* 2016; **294**: 292-300.
[4] Lai K, Lim S, Teh P. Optimization of electrostatic separation process for maximizing biowaste recovery using Taguchi method and ANOVA. *Polish Journal of Environmental Studies* 2015; **24(3)**: 1125-1131.
[5] Manyoma P, Orejuela JP, Torres P, Marmolejo LF, Vidal CJ. Landfill location with expansion possibilities in developing countries. *International Journal of Industrial Engineering* 2015; **22(2)**: 233-241.
[6] Medles K, Dascalescu L, Tilmatine A, Bendaoud A, Younes M. Experimental modeling of the electrostatic separation of granular materials. *Particulate Science and Technology* 2007; **25(2)**: 163-171.
[7] Dascalescu L, Tilmatine A, Aman F, Mihailescu M. Optimization of electrostatic separation processes using response surface modeling. *IEEE Transactions on Industry Applications* 2004; **40(1)**: 53-59.
[8] Jiang W, Jia L, Zhen-Ming X. A new two-roll electrostatic separator for recycling of metals and nonmetals from waste printed circuit board. *Journal of Hazardous Materials* 2009; **161(1)**: 257-262.
[9] Bilici M, Dascalescu L, Barna V, Gyorgy T, Rahou F, Samuila A., 2011. "Experimental modeling of the tribo-aero-electrostatic separation of mixed granular plastics," IEEE Industry Applications Society Annual Meeting (IAS), p. 1–6.
[10] Aryafard E, Farsi M, Rahimpour MR, Raeissi S. Modeling electrostatic separation for dehydration and desalination of crude oil in an industrial two-stage desalting plant. *Journal of the Taiwan Institute of Chemical Engineers* 2016; **58**: 141-147.
[11] Tripathy SK, Ramamurthy Y, Kumar CR. Modeling of high-tension roll separator for separation of titanium bearing minerals. *Powder Technology* 2010, **201(2)**: 181-186.
[12] Giwa A, Daer S, Ahmed I, Marpu PR, Hasan SW. Experimental investigation and artificial neural networks ANNs modeling of electrically-enhanced membrane bioreactor for wastewater treatment. *Journal of Water Process Engineering* 2016; **11**: 88-97.
[13] Lu H, Li J, Guo J, Xu Z. Movement behavior in electrostatic separation: Recycling of metal materials from waste printed circuit board. *Journal of Materials Processing Technology* 2008; **197**: 101-108.
[14] Younes M, Tilmatine A, Medles K, Rahli M, Dascalescu L. Numerical modeling of conductive particle trajectories in roll-type corona-electrostatic separators. *IEEE Transactions on Industry Applications* 2007; **43(5)**: 1130-1136.
[15] Chairez I, García-Peña I, Cabrera A. Dynamic numerical reconstruction of a fungal biofiltration system using differential neural network. *Journal of Process Control* 2009; **19(7)**: 1103-1110.
[16] Esfandian H, Samadi-Maybodi A, Parvini M, Khoshandam B. Development of a novel method for the removal of diazinon pesticide from aqueous solution and modeling by artificial neural networks (ANN). *Journal of Industrial and Engineering Chemistry* 2016; **35**: 295–308.